JOURNAL OF SOLID STATE CHEMISTRY 82, 115–121 (1989)

$In_{1.2}Ga_{0.8}MgO_4$: Powder Neutron Refinement and Crystal Chemistry

JACQUES BARBIER

Department of Chemistry, McMaster University, Hamilton, Ontario, Canada L8S 4M1

Received January 30, 1989; in revised form May 12, 1989

The crystal structure of $YbFe_2O_4$-type $In_{1.2}Ga_{0.8}MgO_4$ has been refined using neutron powder data. The hexagonal parameters of its rhombohedral unit cell are $a = 3.3243(4)$, $c = 25.954(3)$ Å, and $Z = 3$. The structure contains In atoms in octahedral coordination and In + Ga + Mg atoms disordered on trigonal bipyramidal sites. It is shown to be simply related to the $YAlO_3$-type $InGaO_3$(II) structure via a crystallographic shear operation, both structures belonging to the n $InGaO_3 \cdot MgO$ homologous series. © 1989 Academic Press, Inc.

I. Introduction

In their recent investigation of phase relations in the In_2O_3–A_2O_3–BO systems (A = Fe, Ga, Al; B = Mg, Mn, Fe, Ni, Co, Cu, Zn), Kimizuka and Takayama (*1*) and Kimizuka and Mohri (*2*) identified several new compounds of $InGaMO_4$ (M = Cu, Co, Mg, Mn, Zn). Based on powder X-ray diffraction data, all these compounds were found to be isostructural with $YbFe_2O_4$, the crystal structure of which had been determined earlier by Kato *et al.* (*3*). The phase $InGaMgO_4$ was also independently identified by Barbier and Hyde (*4*) in the course of their study of the effect of In/Ga substitution on the stability of the spinelloid phase $Mg_3Ga_2GeO_8$.

The present work reports the structural refinement of the related phase $In_{1.2}Ga_{0.8}MgO_4$ based on powder neutron diffraction data. Its crystal chemistry is discussed in terms of atom close-packing and also in terms of its structural relation to the high-pressure phase $InGaO_3$(II) characterized by Shannon and Prewitt (*5*).

2. Experimental

The compound $In_{1.2}Ga_{0.8}MgO_4$ was synthesized in powder form from a stoichiometric mixture of high-purity MgO, Ga_2O_3, and In_2O_3 powders, sintered in several steps at temperatures between 1100 and 1400°C.

The indium and gallium contents of the final product were determined by neutron activation analysis and the measured In/Ga atomic ratio (1.50(5)) was found to be consistent with the nominal composition $In_{1.2}Ga_{0.8}MgO_4$.

The single-phase nature of the product was also checked by powder X-ray diffraction with a Guinier-Hägg camera ($CuK\alpha_1$ radiation, Si internal standard). The X-ray powder pattern of $In_{1.2}Ga_{0.8}MgO_4$ is given in Table I: it is indexed on a rhombohedral unit cell with the hexagonal parameters $a = 3.3259(2)$, $c = 25.962(3)$ Å, and $Z = 3$. As expected from the higher indium content, this unit cell is slightly larger than that reported by Kimizuka and Mohri (*2*) for $InGaMgO_4$, viz., $a = 3.3036$, $c = 25.805$ Å.

0022-4596/89 $3.00

TABLE I

POWDER X-RAY DIFFRACTION PATTERN (GUINIER-HÄGG CAMERA) OF $In_{1.2}Ga_{0.8}MgO_4$ INDEXED ON THE FOLLOWING RHOMBOHEDRAL UNIT CELL: a = 3.3259(2), c = 25.962(3) Å, Z = 3 (HEXAGONAL AXES)

h k l	d_{cal} (Å)	d_{obs} (Å)	I_{obs}
0 0 3	8.654	8.651	61
0 0 6	4.327	4.330	41
0 0 9	2.8847	2.8855	100
1 0 1	2.8628	2.8623	
0 1 2	2.8120	2.8126	<1
1 0 4	2.6327	2.6343	93
0 1 5	2.5188	2.5190	73
1 0 7	2.2749	2.2755	10
0 0 12	2.1635	—	—
0 1 8	2.1542	2.1547	19
1 0 10	1.9285	1.9287	49
0 1 11	1.8256	—	—
0 0 15	1.7308	1.7310	2
1 1 0	1.6630	1.6629	34
1 0 13	1.6412	1.6410	15
1 1 3	1.6331	1.6333	<1
0 1 14	1.5592	1.5595	32
1 1 6	1.5523	1.5521	19
0 0 18	1.4424	—	—
1 1 9	1.4407	1.4410	35
0 2 1	1.4379	1.4377	
2 0 2	1.4314	—	—
1 0 16	1.4137	—	—
0 2 4	1.4060	1.4061	14
2 0 5	1.3878	1.3878	7
0 1 17	1.3493	1.3493	3
0 2 7	1.3425	1.3428	<1
1 1 2	1.3185	—	—
2 0 8	1.3164	1.3166	4
0 2 10	1.2594	1.2594	6
0 0 21	1.2363	—	—
1 0 19	1.2346	1.2346	2
2 0 11	1.2294	—	—
1 1 15	1.1992	1.1990	5
0 1 20	1.1835	—	—
0 2 13	1.1681	1.1677	3
2 0 14	1.1374	1.1373	10

Note. All calculated lines up to 2θ = 85° have been included in the pattern. I_{obs} represent integrated intensities recorded with a Nicolet I2 diffractometer.

This result indicates the existence of a composition range (in terms of In/Ga substitution) for the $InGaMgO_4$ compound, but no attempt has been made in the present study to determine it more precisely.

Neutron powder data were collected at the McMaster Nuclear Reactor using a 6-g sample of $In_{1.2}Ga_{0.8}MgO_4$ powder contained in a thin-walled vanadium can and 1.3916-Å neutrons obtained from a [200] copper monochromator. The diffraction data were recorded at room temperature over the angular range $20 < 2\theta < 100°$ at four different settings of the position-sensitive detector which is essentially the same as that in use at Missouri University Research Reactor (MURR) which has been described previously (*6*). Soller-type collimators are not currently used but an oscillating–rotating collimator is in place between the sample and the detector to reduce background levels. The resolution of the McMaster instrument is similar to that of the facility at MURR but FWHM values for standard materials are 20–25% greater in the same 2θ range. After correction of the raw data for detector geometry (*6*), the profile refinement was carried out with a local version of the Rietveld program. Scattering lengths of 0.538, 0.407, 0.729, and 0.581 were used for Mg, In, Ga, and O nuclei, respectively (*7*).

3. Structure Refinement

The refinement of the $In_{1.2}Ga_{0.8}MgO_4$ structure was started using the cell parameters determined by powder X-ray diffraction (cf. above) and the atomic positions determined by Kato *et al.* (*3*) for the isostructural $YbFe_2O_4$ compound (with In on the Yb site (3a) and (0.1 In + 0.4 Ga + 0.5 Mg) on the Fe site (6c) of the $R\bar{3}m$ space group).

The structural parameters allowed to vary during the refinement included the cell parameters, the atomic coordinates, and the isotropic temperature factors. The re-

finement converged smoothly to a weighted profile Rwp index of 6.5% and a nuclear Rn index (corresponding to the Bragg peak intensity) of 3.5% (for an expected Re index of 2.1%). The final positional and thermal parameters are listed in Table II and the observed, calculated, and difference profiles are shown in Fig. 1.

A few more cycles of refinement were attempted in which some In/Ga or In/Mg disorder was introduced on the 3a site: this, however, did not alter the final Rwp index significantly and even resulted in a slightly larger Rn index. It is therefore concluded that the 3a site is occupied by In only while the 6c site has a Ga/Mg/In mixed occupancy. As discussed below, this cation distribution is consistent with the observed coordination geometry around the metal sites.

4. Description of the $In_{1.2}Ga_{0.8}MgO_4$ Structure

The crystal structure of the $In_{1.2}Ga_{0.8}MgO_4$ compounds is shown Fig. 2 projected on the $[11\bar{2}0]_{hex}$ plane. Selected bond lengths and angles are given in Table III. Associated bond strengths have been calculated from the empirical parameters of Altermatt and Brown (*8*).

As in the case of the isostructural Yb Fe_2O_4 (*3*), the structure can be described as a close-packing of oxygen atoms with metal atoms in octahedral ($M(1)$ = In) and trigo-

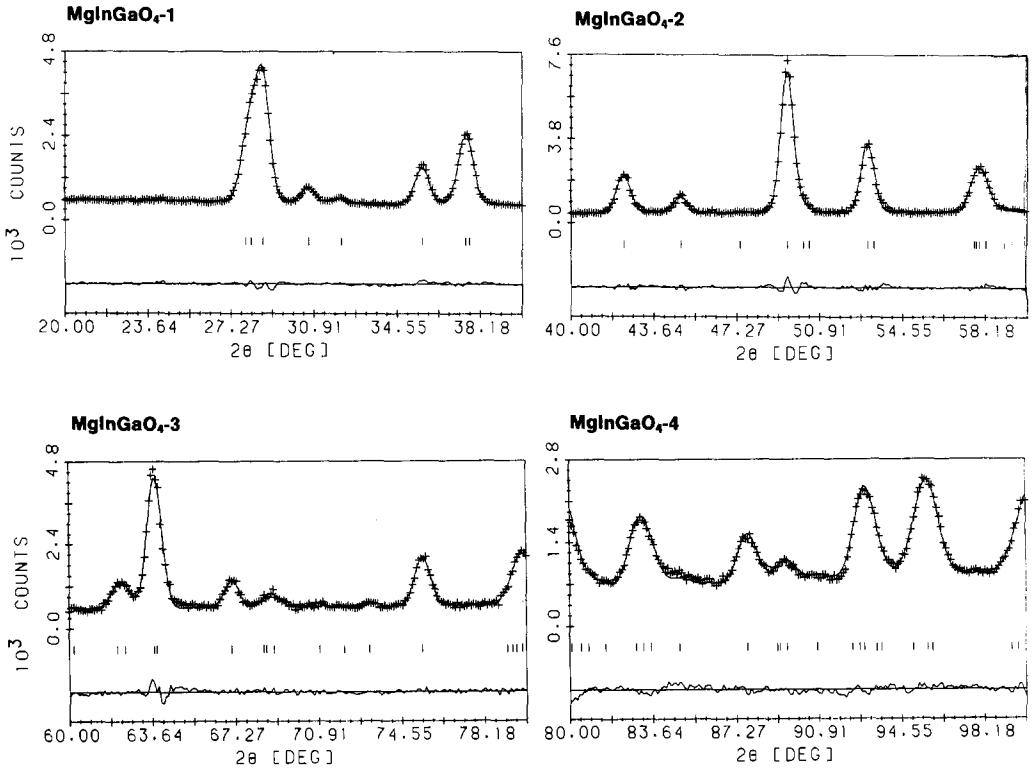

FIG. 1. Plots of the observed (+), calculated (solid line), and difference (bottom) neutron intensity profiles obtained for $In_{1.2}Ga_{0.8}MgO_4$ over the angular range 20–100° (2θ). The short vertical bars indicate the positions of the Bragg peaks. The four frames correspond to the four positions of the position-sensitive detector used for collecting the data.

TABLE II

FINAL ATOMIC POSITIONS, ISOTROPIC TEMPERATURE FACTORS, AND AGREEMENT INDICES FOR THE NEUTRON POWDER REFINEMENT OF $In_{1.2}Ga_{0.8}MgO_4$

Atom	x	y	z	B(Å^2)
$M(1)^a$ (3a)	0	0	0	0.43(12)
$M(2)^a$ (6c)	0	0	0.2164(2)	0.51(7)
O(1) (6c)	0	0	0.2929(2)	0.38(7)
O(2) (6c)	0	0	0.1286(1)	1.01(8)

Weighted profile index, Rwp	= 6.5%
Nuclear index, Rn	= 3.5%
Expected Index, Re	= 2.1%
Number of data points	= 804
Number of reflections	= 69
Number of variables	= 22
Number of degrees of freedom	= 782

Note. The hexagonal cell parameters are a = 3.3243(4), c = 25.954(3) Å, Z = 3, $R\bar{3}m$ space group. The estimated standard deviations on the last digit are given in parentheses.

[a] $M(1)$ = In; $M(2)$ = 0.1 In + 0.4 Ga + 0.5 Mg.

nal bipyramidal ($M(2)$ = 0.1 In + 0.4 Ga + 0.5 Mg) coordination. The oxygen array forms a 12-layer mixed stacking of cubic and hexagonal layers corresponding to the sequence $(h^2c^2)^3$.

It is noteworthy, however, that the observed c/a ratio (7.807) is very much smaller than the ideal value $12\sqrt{\frac{2}{3}}$ = 9.798 expected for a 12-layer close-packed structure. As seen in Fig. 2, this squashing of the oxygen array along the c direction is particularly pronounced in the InO_6 octahedral layers with O–In–O bond angles deviating by as much as 9° from their ideal values of 90° (cf. Table III). The six identical In–O bond lengths (2.187 Å) are nevertheless in good agreement with the value of 2.18 Å predicted from Shannon's ionic radii (*9*). A very similar indium coordination was also found by Shannon and Prewitt (*5*) in the structure of the related compound $InGaO_3$(II) shown in Fig. 3.

The metal atoms in the $M(2)$ site are bonded to five oxygen atoms at the corners of a rather regular trigonal bipyramid with three equatorial bonds of equal length (1.943 Å) plus one short (1.985 Å) and one long (2.280 Å) axial bond (cf. Table III). The unequal axial bonds result from the off-center position of the $M(2)$ atoms which, in turn, can be associated with strong $M(2)$–

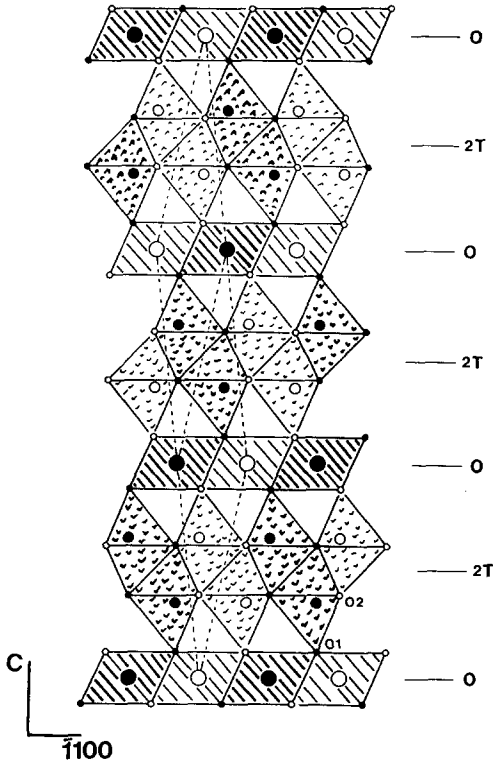

FIG. 2. The crystal structure of $In_{1.2}Ga_{0.8}MgO_4$ projected on the $(11\bar{2}0)$ plane of the hexagonal cell. The true symmetry is rhombohedral and a unit cell is outlined in the drawing. Large, medium, and small circles represent $M(1)$, $M(2)$, and oxygen atoms, respectively. Open and filled circles are at heights 0 and 50 (in units of $\frac{1}{100}$ of the repeat distance, $d_{11\bar{2}0}$ = 3.32 Å). The structure consists in a stacking in the c-direction of octahedral layers (O) (edge-sharing $M(1)O_6$ octahedra) alternating with double trigonal bipyramidal layers (2T) (edge- and corner-sharing $M(2)O_5$ bipyramids). Note the squashing of the $M(1)O_6$ octahedra and the off-center positions oif the metal atoms in the $M(2)O_5$ bipyramids. All oxygen atoms are tetrahedrally coordinated. Compare with the $InGaO_3$(II) structure depicted in Fig. 3.

TABLE III

SELECTED BOND LENGTHS (l IN Å), BOND STRENGTHS (s), AND ANGLES (IN DEG) IN THE $In_{1.2}Ga_{0.8}MgO_4$ STRUCTURE

InO_6 octahedron	l	s
In–O(1)	2.187(2) (×6)	0.463 (×6)
		Σs = 2.78
$O(1)^{i}$–In–$O(1)^{ii}$		98.9(1)
$O(1)^{i}$–In–$O(1)^{iii}$		81.1(1)
$M(2)O_5$ trigonal bipyramid	l	s^a
$M(2)$–O(2)	1.9432(4) (×3)	0.569 (×3)
$M(2)$–O(1)	1.985(4)	0.508
$M(2)$–O(2)	2.280(3)	0.229
Mean	2.019	$\Sigma\bar{s}$ = 2.44
O(2)–$M(2)$–$O(2)^{iv}$		80.99(8)
O(1)–$M(2)$–$O(2)^{iv}$		99.01(8)
$O(2)^{iv}$–$M(2)$–$O(2)^{v}$		117.60(4)

Note. The estimated standard deviations on the last digit are given in parentheses. Symmetry code: (i) $-\frac{2}{3}+x, -\frac{1}{3}+y, -\frac{1}{3}+z$; (ii) $\frac{1}{3}+x, -\frac{1}{3}+y, -\frac{1}{3}+z$; (iii) $\frac{2}{3}+x, \frac{1}{3}+y, \frac{1}{3}-z$; (iv) $-\frac{1}{3}+x, -\frac{2}{3}+y, \frac{1}{3}-z$; (v) $-\frac{1}{3}+x, \frac{1}{3}+y, \frac{1}{3}-z$.

[a] s is the "weighted" bond strength according to occupancy of the $M(2)$ site, i.e., (0.1 In + 0.4 Ga + 0.5 Mg) with an average cation valence of 2.5.

$M(2)$ repulsions across the edge shared by adjacent $M(2)O_5$ trigonal bipyramids. Indeed, in the related $InGaO_3$(II) structure containing single layers of GaO_5 trigonal bipyramids only (Fig. 3), the Ga atoms occupy central positions with two identical Ga–O axial bonds (*5*). A similar effect also occurs in the $Yb_2Fe_3O_7$ structure (*10*) containing single and double layers of FeO_5 trigonal bipyramids. Taking into account the mixed occupancy of the $M(2)$ site (0.1 In + 0.4 Ga + 0.5 Mg), weighted bond strengths can be calculated for individual $M(2)$–O bonds resulting in a bond strength sum of 2.44 in good agreement with the average cation valence of 2.5 (cf. Table III).

Examples of crystal structures containing five-coordinated Mg, Ga, or In atoms are apparently uncommon but include, for instance, $Mg_3(PO_4)_2$ (*11*), $InGaO_3$(II) (*5*), and hexagonal $LnInO_3$ (Ln = Eu, Gd, Tb, Dy, Ho, Y) (*12*). The $YInO_3$ structure is a distorted variant of the $InGaO_3$(II) and $YAlO_3$ (*13*) structures and contains In atoms in a strongly distorted trigonal bipyramidal coordination. Interestingly, it is unstable at high temperature and transforms above 1000°C into a C-type rare-earth oxide structure with six-coordinated cations only (*12*). By analogy, the presence of some five-coordinated In atoms in the $In_{1.2}Ga_{0.8}MgO_4$ structure might be associated with its sluggish decomposition when heated for several days at 1600°C in a sealed Pt tube.

All the oxygen atoms in the $In_{1.2}Ga_{0.8}MgO_4$ structure are tetrahedrally coordinated: O(1) to one $M(2)$ and three $M(1)$ at-

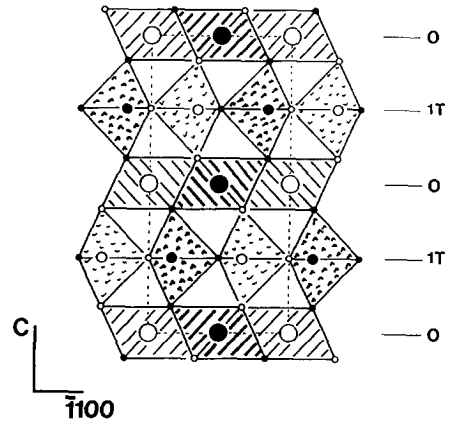

FIG. 3. The crystal structure of $InGaO_3$(II) (*5*) projected on the $(11\bar{2}0)$ plane. Large, medium, and small circles represent In, Ga, and O atoms, respectively. Open and filled circles are at heights 0 and 50 (in units of $\frac{1}{100}$ of the repeat distance, $d_{11\bar{2}0}$ = 3.31 Å). The structure contains octahedral layers (edge-sharing InO_6 octahedra) alternating in the c-direction with single trigonal bipyramidal layers (1T) (corner-sharing GaO_5 bipyramids). Note that the InO_6 octahedra are squashed and that the Ga atoms occupy the centers of the bipyramids. The oxygen atoms are three- and four-coordinated by the metal atoms. The relation to the $In_{1.2}Ga_{0.8}MgO_4$ structure in Fig. 2 is obvious.

oms and O(2) to four $M(2)$ atoms with bond strength sums of 1.90 and 1.94, respectively (cf. Fig. 2 and Table III). The larger thermal parameter of the O(2) atom (cf. Table II) can, perhaps, be linked to the presence of a longer (2.280 Å), weaker O(2)–$M(2)$ bond parallel to the c direction. The overall coordination of the $In_{1.2}Ga_{0.8}MgO_4$ structure can then be written as $^{VI}In^{V}(In_{0.2}Ga_{0.8}Mg)^{IV}O_4$.

Interestingly, as has been pointed out by Professor B. G. Hyde (private communication), this structure can alternatively be described in terms of a metal close-packing "stuffed" with oxygen atoms in the tetrahedral sites, the oxygen positions being such as to satisfy their bonding requirements (thus, explaining the displacement of the O(2) atom along the c-direction toward an $M(2)$ and away from an $M(1)$ metal atom). As seen in Fig. 2, the metal atom layers correspond to the stacking sequence $(ch^2)^3$, i.e., a 9-layer close-packed structure. And indeed, the observed c/a ratio (7.807) is much closer to that expected for a 9-layer cation close-packing ($9\sqrt{\frac{2}{3}} = 7.348$) than that corresponding to a 12-layer oxygen close-packing ($12\sqrt{\frac{2}{3}} = 9.798$). The same observation applies to all isostructural or related compounds (e.g., n $YbFeO_3 \cdot FeO$ (n = 1, 2, 3, 4), $InGaO_3$(II), $YAlO_3$, $YInO_3$) showing that, in all cases, the metal atom packing is much more regular (close-packed) than the oxygen packing. A similar conclusion was also reached by O'Keeffe and Hyde (*14*) in their description of the A-La_2O_3 and Th_3N_4 structures.

5. Relation to the $InGaO_3$(II) Structure

$InGaO_3$(II) has been characterized as a high-pressure phase in the In_2O_3–Ga_2O_3 system by Shannon and Prewitt (*5*). Its crystal structure ($P6_3/mmc$, a = 3.310, c = 12.039 Å, Z = 2) is depicted in Fig. 3 projected on the $(11\bar{2}0)$ plane. It is based on a mixed cubic-hexagonal oxygen packing with the layer sequence $(hc^2)^2$, i.e., a six-layer structure. [Note that, again, the c/a ratio (3.637) is much less than the expected value $6\sqrt{\frac{2}{3}} = 4.899$.] In and Ga atoms are six- and five-coordinated, respectively, and layers of edge-sharing InO_6 octahedra alternate in the c direction with layers of corner-sharing GaO_5 trigonal bipyramids.

The relation between the $InGaMgO_4$ and $InGaO_3$(II) structures is straightforward, corresponding to the replacement of double layers of (Ga, Mg)O_5 bipyramids in the former by single layers of GaO_5 bipyramids in the latter (compare Figs. 2 and 3). This structural relationship can then be formally expressed as $InGaMgO_4 = InGaO_3 + MgO$ and the transformation $InGaMgO_4 \rightarrow InGaO_3$ would simply involve the elimination of an MgO layer via a crystallographic shear operation. [It is noteworthy that an analogous relationship has been previously described in the case of the spinel and β-Ga_2O_3 structures, i.e., $MgGa_2O_4$ spinel = β-Ga_2O_3 + MgO (*15*).] The $InGaMgO_4$ and $InGaO_3$(II) structures therefore represent the members $n = 1$ and $n = \infty$ of a n $InGaO_3 \cdot MgO$ homologous series similar to the n $YbFeO_3 \cdot FeO$ series of ytterbium–iron oxides for which the members n = 1, 2, 3, and 4 have been characterized (*16*). The present work also indicated the existence of other phases in the n $InGaO_3 \cdot MgO$ structural family: examination by electron diffraction/microscopy of a $In_{1.2}Ga_{0.8}MgO_4$ sample quenched from 1600°C showed the formation of disordered microscopic intergrowths including, in particular, a new hexagonal phase with approximate cell parameters a = 3.30 and c = 39.3 Å.

A minor difference between the $InGaMgO_4$ and $InGaO_3$(II) structures is the absence of a composition range for the latter as reported by Shannon and Prewitt (*5*). This could, perhaps, be attributed to the large difference between the In–O and Ga–O bond lengths precluding the mixed occupancy of sites in the $InGaO_3$(II) structure. [The room-pressure $InGaO_3$ phase has the

β-Ga_2O_3 structure with In and Ga atoms probably ordered on the octahedral and tetrahedral sites, respectively (*5*).] However, the presence of Mg atoms in the $M(2)O_5$ bipyramids of the $InGaMgO_4$ structure enlarges the average size of these sites ($\langle M(2)\text{–}O\rangle$ = 2.02 Å vs Ga–O = 1.94 Å in $InGaO_3$(II)), thereby allowing some In/Ga substitution to occur.

The formation of the $InGaO_3$(II) structure at high pressure is consistent with the increased coordination of the Ga atoms (from IV to V) and with the 4.8% density increase accompanying the β-$InGaO_3 \rightarrow$ $InGaO_3$(II) transition (*5*). On the other hand, the formation of the $InGaMgO_4$ structure at 1 atm in the $MgIn_2O_4$–$MgGa_2O_4$ system is unexpected: both end-members adopt a predominantly inverse spinel structure (*17*) and a continuous $Mg(In, Ga)_2O_4$ spinel solid solution might have been expected. It has been found in the present work that a spinel phase in equilibrium with $InGaMgO_4$ has a cell parameter of 8.445(2) Å. Assuming that Vegard's law holds for the $MgIn_2O_4$–$MgGa_2O_4$ system, this cell dimension corresponds to a solubility limit of 30 mol% $MgIn_2O_4$ (i.e., $MgGa_{1.4}In_{0.6}O_4$) in $MgGa_2O_4$ spinel at 1400°C. This is intermediate between the composition ranges of the spinel phases in the Co system (up to $CoGa_{1.6}In_{0.6}O_4$ at 1300°C (*1*)) and in the Ni system (no $YbFe_2O_4$-type phase has been observed and $NiGaInO_4$ crystallizes with a spinel structure at 1400°C (*2*)).

Acknowledgments

The author is grateful to Mr. J. Reimers for his help with the neutron diffraction experiment. The financial support from the Canadian National Science & Engineering Research Council is also acknowledged.

References

1. N. KIMIZUKA AND E. TAKAYAMA, *J. Solid State Chem.* **53,** 217 (1984).
2. N. KIMIZUKA AND T. MOHRI, *J. Solid State Chem.* **60,** 382 (1985).
3. K. KATO, I. KAWADA, AND N. KIMIZUKA, *Z. Kristallogr.* **141,** 314 (1975).
4. J. BARBIER AND B. G. HYDE, *Phys. Chem. Miner.* **13,** 382 (1986).
5. R. D. SHANNON AND C. T. PREWITT, *J. Inorg. Nucl. Chem.* **30,** 1389 (1968).
6. C. W. TOMPSON, D. F. R. MILDNER, M. MEHREGANG, J. SUDOL, R. BERLINER, AND W. B. YELON, *J. Appl. Crystalogr.* **17,** 385 (1984).
7. V. F. SEARS, "Thermal Neutron Scattering Lengths and Cross-sections for Condensed Matter Research," Atomic Energy of Canada Limited, Report AECL-8490 (1984).
8. D. ALTERMATT AND I. D. BROWN, *Acta Crystallogr. Sect. B* **41,** 240 (1985).
9. R. D. SHANNON, *Acta Crystallogr. Sect. A* **32,** 751 (1976).
10. K. KATO, I. KAWADA, N. KIMIZUKA, AND I. SHINDO, *Z. Kristallogr.* **143,** 278 (1976).
11. A. G. NORD AND P. KIERKEGAARD, *Acta Chem. Scand.* **22,** 1466 (1968).
12. C. W. F. T. PISTORIUS AND G. J. KRUGER, *J. Inorg. Nucl. Chem.* **38,** 1471 (1976).
13. F. BERTAUT AND J. MARESCHAL, *C. R. Acad. Sci.*, 867 (1963).
14. M. O'KEEFFE AND B. G. HYDE, *Struct. Bonding* **61,** 77 (1985).
15. J. BARBIER AND B. G. HYDE, *Acta Crystallogr. Sect. B* **43,** 34 (1987).
16. N. KIMIZUKA, K. KATO, I. SHINDO, AND I. KAWADA, *Acta Crystallogr. Sect. B* **32,** 1620 (1976).
17. R. J. HILL, J. R. CRAIG, AND G. V. GIBBS, *Phys. Chem. Miner.* **4,** 317 (1979).